Advanced Composite Materials
Publication details, including instructions for authors and subscription information:
http://www.tandfonline.com/loi/tacm20

Eccentric compression bending test for CFRP pipe

Hiroshi Fukuda , Osamu Watanabe , Masaaki Itabashi & Atsushi Wada

Version of record first published: 02 Apr 2012.

Adv. Composite Mater., Vol. 11, No. 2, pp. 193–201 (2002)

Eccentric compression bending test for CFRP pipe

HIROSHI FUKUDA*, OSAMU WATANABE, MASAAKI ITABASHI and ATSUSHI WADA

Department of Materials Science and Technology, Tokyo University of Science, 2641 Yamazaki, Noda, Chiba 278-8510, Japan

Received 5 March 2002; accepted 17 April 2002

Abstract—This paper reports a new test method to evaluate the bending strength of composite pipes. In the past, we proposed a compression bending test method to get more reliable bending strength values than the conventional three- or four-point bending test. This compression bending was successfully applied not only to flat CFRP coupons but also to slender CFRP pipes. However, if the diameter of the pipe is relatively large, this compression bending is not necessarily appropriate. Therefore, as a step forward to accurate determination of compression bending, an eccentric compression bending test method is tried in the present paper.

Keywords: CFRP pipe; eccentric compression bending; bending strength; failure pattern.

1. INTRODUCTION

It is well known that the bending strength of a CFRP coupon is strongly affected by the stress concentration due to a hard loading device. The works of Whitney [1] and Cui and Wisnom [2] are some examples to have dealt with this stress concentration.

To compensate for this undesirable effect, the authors have hitherto proposed and demonstrated a compression bending test method [3–6] which is based on Euler buckling of a column. If we measure only the applied load and the crosshead movement during the buckling process of the column, we can calculate both the bending strength and the bending modulus applying the elastica [7].

The above undesirable effect of the loading device used for 3- or 4-point bending will be more serious for CFRP pipes; in most cases, the pipe will be crushed by the loading nose rather than through a bending failure. Then, as a second step, we tried to apply this compression bending test to several kinds of CFRP pipes [8]. Again it was demonstrated that the bending strength by means of the compression bending was larger than that measured by the 3-point bending.

*To whom correspondence should be addressed. E-mail: fukuda@rs.noda.tus.acjp

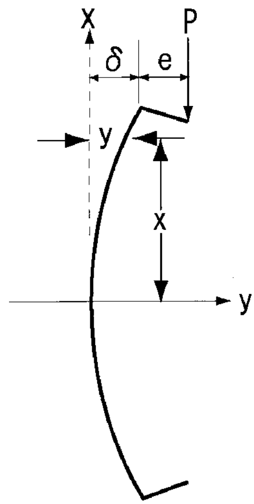

Figure 1. Eccentric compression bending.

During a series of tests in ref. [8], another difficulty arose: if the diameter of the pipe is large, Euler buckling is less likely to occur. Then, as a successive work, we tried a bending by means of eccentric compression as shown in Fig. 1.

In the present paper, the results of the eccentric compression bending test and the advantage of this method will be presented.

2. PRINCIPLE OF ECCENTRIC COMPRESSION BENDING

In the case of eccentric compression bending illustrated in Fig. 1, the bending moment of an arbitrary point is [9]

$$M_x = P(e + \delta - y), \tag{1}$$

and the maximum bending moment at the center of the pipe is

$$M_{\max} = P(e + \delta). \tag{2}$$

Then the maximum bending stress (skin stress at the midspan) is

$$\sigma_{\max} = \frac{M_{\max}}{Z}, \tag{3}$$

where Z is the section modulus of the pipe. If the axial compressive stress should be taken into account,

$$\sigma_{\max} = \frac{M_{\max}}{Z} + \frac{P}{A}, \tag{4}$$

is the maximum stress, where A is the cross-sectional area of the pipe. Equation (4) can be understood as the maximum compressive stress at failure.

3. SPECIMEN AND TEST PROCEDURE

3.1. Test specimens

All specimens tested here are CFRP pipes where carbon prepregs with longitudinal and transverse direction are wound on a cylindrical mandrel as is shown schematically in Fig. 2. Three kinds of pipes were used for this test — these are, Type A: two plies of 0.10 mm-thick longitudinal prepreg and 0.02 mm-thick transverse prepreg giving a total thickness of about 0.25 mm; Type B: four plies of the same prepreg as Type A, which means the wall thickness is double, about 0.50 mm; Type C: four plies of thinner prepregs with total thickness of *ca.* 0.25 mm. The Type C specimens are the same as in the previous work [8] and the prepreg used for Type C specimens is different from that of Type A or Type B specimens. The inner diameter of every pipe was fixed at 15 mm against the previous work that used 3, 5, 15 mm diameters [8], because this test was mainly focused on relatively large-diameter pipes. Table 1 summarizes these three kinds of specimens.

3.2. Eccentric compression bending test

Figure 3 is a schematic view of the device for the eccentric compression bending. To realize compressive load plus bending moment at the ends of specimen, we designed and machined this pair of special fixtures. Each end of the pipe is inserted and fixed to each hole of the rotation-free arm. By using this device, bending moment (applied load times arm length) can be applied at both ends of the specimen. The arm length is denoted as eccentricity, e, hereafter. Most of the eccentric compression bending tests were performed at the crosshead speed of 5 mm/min. The specimen length was either 500, 600 or 700 mm and the eccentricity of 0, 10, 20, 30, 40 or 50 mm was tested. At least 5 specimens were tested at each condition. In the experiment, the applied load was measured with a load cell attached to an Instron-type testing machine and the midspan deflection was measured with a displacement transducer. These data were saved in a personal computer at the time interval of one second.

4. RESULTS AND DISCUSSION

4.1. Apparent bending strength

Figures 4–6 summarize the relations between the bending strength and the eccentricity of Types A, B and C specimens where the failure stress is calculated by equation (4). Each symbol indicates the average and each vertical range shows the standard deviation. Data of various specimen lengths are also shown in these figures.

According to Fig. 4 for Type A specimens, the failure stress tends to decrease with increasing eccentricity. This result is somewhat strange because the bending strength should be the same regardless of different arm length, e. This indicates that

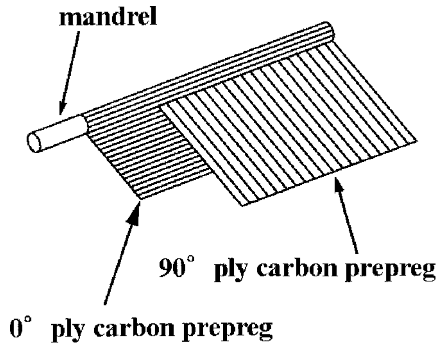

Figure 2. Fabrication of CFRP pipe.

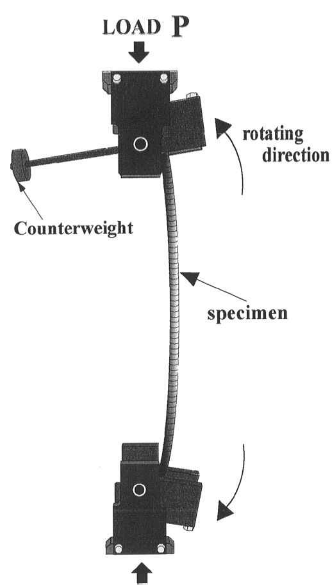

Figure 3. Schematic view of eccentric compression bending.

Table 1.
Prepregs and specimen configuration

Type	Prepreg weight content (g/m^2)				Pipe		
	0° direction		90° direction		Number of plies	Thickness (mm)	E (GPa)
	CF	Resin	CF	Resin			
A	108	57	19	19	2	0.26	108
B	108	57	19	19	4	0.54	108
C	54	23	19	19	4	0.28	77.3

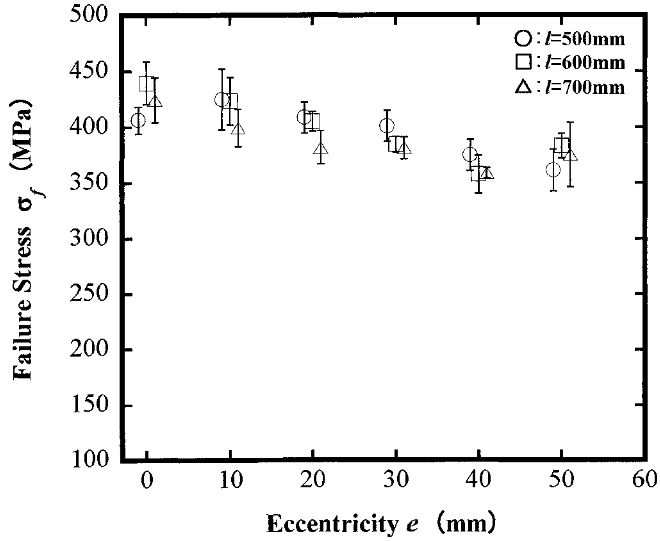

Figure 4. Failure stress *vs.* eccentricity (Type A).

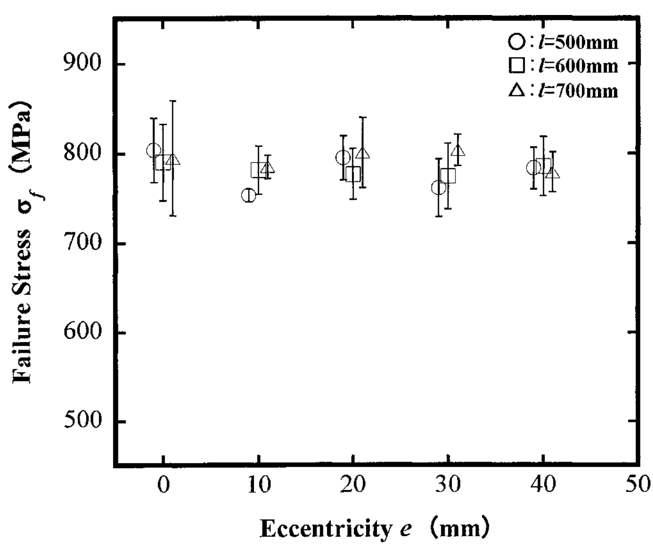

Figure 5. Failure stress *vs.* eccentricity (Type B).

the failure pattern is not a bending failure and this strange result will be discussed later. The effect of the specimen length was not clear.

As for Type B (Fig. 5) and Type C (Fig. 6) specimens, no obvious relationship between strength and eccentricity was observed. This indirectly suggests that the failure takes place at the compressive side of each specimen for Type B and Type C specimens.

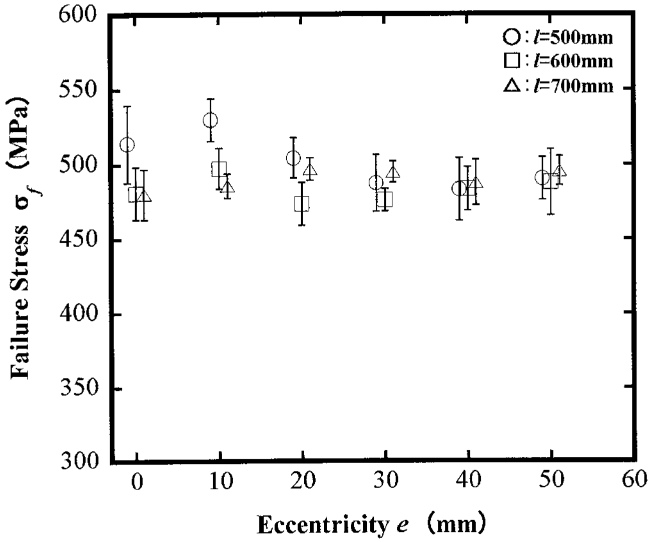

Figure 6. Failure stress *vs.* eccentricity (Type C).

4.2. Discussion of the failure pattern and bending strength

To make clear the above strange result of Type A specimens, we observed the failure pattern. Figure 7 is a typical example of failure patterns of Type A and Type B specimens. The failure pattern of Type C specimens was close to that of Type B specimens. All Type A specimens showed longitudinal splitting and load-bearing capacity decreased. They did not separate into two pieces. As was described in Section 3.1, the number of fibers in the longitudinal direction is more than 5 times that in the transverse (hoop) direction. The failure mechanism of generating splitting may be understood as follows: under the bending moment, a flattening of the cross-section from circular shape to elliptical shape takes place; due to this flattening, carbon fibers in the hoop direction break; finally longitudinal splitting occurs.

In the case of Type B specimens, even though the same prepregs as in Type A were used, the longitudinal splitting could not be observed. Because the wall thickness was large, the flattening of the cross-section could hardly occur and hence, the apparent bending failure (failure at the compression side) occurred.

The bending failure of Type C specimens can be understood as follows. Although the wall thickness is the same as in Type A specimens, the amount of fibers in the circumference is more than in Type A specimens. Therefore, the compressive failure took place prior to longitudinal splitting, even though some flattening of the cross-section might have occurred. This result can be used for optimum design of CFRP pipes.

To confirm the above assumption, we next evaluated the data of Type A specimens by using equation (3), instead of equation (4). This evaluation is based on the idea that the flattening of a pipe is due to the applied bending moment, not compressive

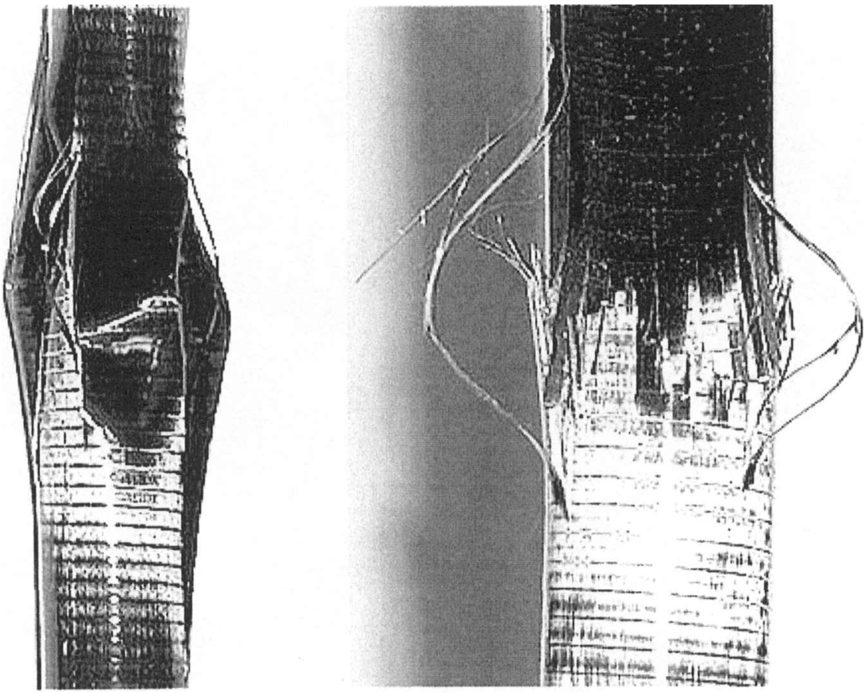

Figure 7. Difference of failure pattern (Type A and B).

stress. Figure 8 shows the result; a rather uniform value is obtained regardless of various values of the eccentricity and this result indirectly confirms that the failure pattern of Type A specimens is splitting. This stress should be understood as skin stress that generates the splitting.

4.3. Ratio of compressive stress to bending stress

The compression bending, even the eccentric compression bending, inevitably includes compressive stress in addition to bending stress. If the ratio of the compressive stress to the bending stress is large, it should no longer be called a bending test. This point was also examined, and Fig. 9 demonstrates the most severe case of thicker specimens (Type B) where σ_{comp} is calculated simply by $\frac{P}{A}$. With increasing eccentricity and specimen length, the ratio decreased, as will be understood. Data at $e = 0$ are the values of compression bending, although tests were conducted using the same fixtures as the eccentric compression bending. Comparing with the compression bending, the eccentric compression bending exhibited smaller ratio of compressive stress to bending stress. Thus, it will be concluded that the present eccentric compression bending test is a step forward

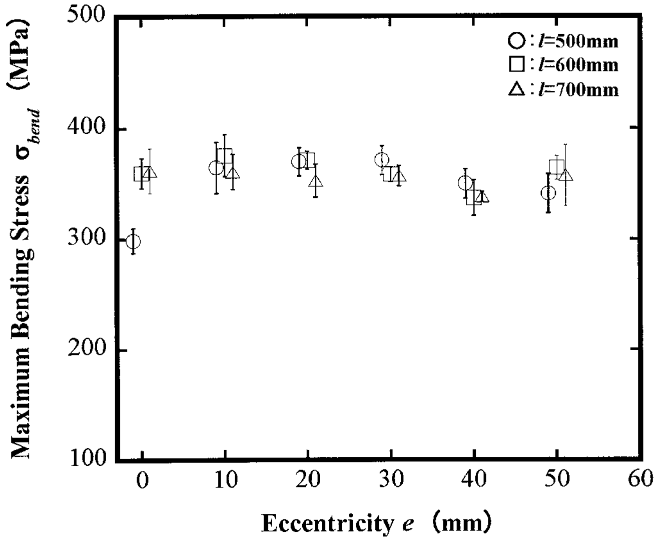

Figure 8. Maximum bending stress *vs.* eccentricity (Type A).

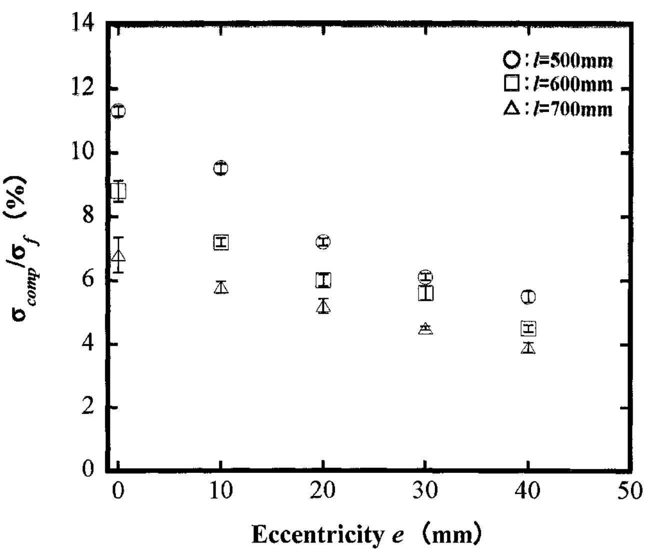

Figure 9. Ratio of compressive stress to failure stress (Type B).

to compression bending evaluation and this method is acceptable from a practical viewpoint.

5. CONCLUSIONS

An eccentric compression bending, a revised version of the compression bending method used previously, was tried against CFRP pipes. For thin-wall pipes, it was rather difficult to generate bending failure whereas fairly good results were obtained for thicker-wall pipes.

Acknowledgements

We sincerely thank Mr. H. Suzue and Mr. K. Kameda of Daiwa Seiko Co. Ltd. for supplying the test specimens. Thanks are also addressed to Mr. I. Watanabe for his assistance in experiments.

REFERENCES

1. J. M. Whitney, Elasticity analysis of orthotropic beams under concentrated loads, *Compos. Sci. Technol.* **22**, 167–184 (1985).
2. W.-C. Cui and M. R. Wisnom, Contact finite element analysis of three- and four-point short-beam bending of unidirectional composites, *Compos. Sci. Technol.* **45**, 323–354 (1992).
3. H. Fukuda, A new bending test method of advanced composites, *Experimental Mechanics* **29**, 330–335 (1989).
4. H. Fukuda, Compression bending test method for advanced composites, *J. Japan Soc. Aero. Space Sci.* **41**, 482–487 (1993) (in Japanese).
5. H. Fukuda, H. Katoh and H. Uesugi, A modified procedure to measure bending strength and modulus of advanced composites by means of compression bending, *J. Compos. Mater.* **29**, 195–207 (1995).
6. H. Fukuda and M. Itabashi, Simplified compression bending test method for advanced composites, *Composites, Part A* **30**, 249–256 (1999).
7. S. P. Timoshenko and J. M. Gere, in: *Theory of Elastic Stability*, 2nd edn, pp. 76–82. McGraw-Hill (1961).
8. H. Fukuda, T. Watanabe and M. Itabashi, Compression bending test method for CFRP pipe, in: *Proc. 2nd Asian-Australasiar Conf. on composite Mater. (ACCM-2000)*, pp. 1187–1192 (2000).
9. S. P. Timoshenko, in: *Strength of Materials*, Part I, 3rd edn, p. 259. Van Nostrand Reinhold (1955).